Conf-910435--67

ANL/CP--71299

DE91 010794

MECHANISTIC INTERPRETATION OF GLASS REACTION: INPUT TO KINETIC MODEL DEVELOPMENT

J. K. BATES, W. L. EBERT
Argonne National Laboratory
9700 South Cass Avenue
Argonne, IL 60439-4837
(708) 972-4385

W. L. BOURCIER
Lawrence Livermore National Laboratory
P. O. Box 808
Livermore, CA 94550
(415) 423-3745

J. P. BRADLEY
McCrone Associates, Inc.
850 Pasquinelli Drive
Westmont, IL 60559
(708) 887-7417

ABSTRACT

Actinide-doped SRL 165 type glass was reacted in J-13 groundwater at 90°C for times up to 278 days. The reaction was characterized by both solution and solid analyses. The glass was seen to react nonstoichiometrically with preferred leaching of alkali metals and boron. High resolution electron microscopy revealed the formation of a complex layer structure which became separated from the underlying glass as the reaction progressed. The formation of the layer and its effect on continued glass reaction are discussed with respect to the current model for glass reaction used in the EQ3/6 computer simulation. It is concluded that the layer formed after 278 days is not protective and may eventually become fractured and generate particulates that may be transported by liquid water.

INTRODUCTION

The goal of the Glass Task in support of the Yucca Mountain Project (YMP) is to develop a methodology to predict the performance of glass waste forms over the lifetime of the repository. Information generated in this Task follows the Glass Scientific Information Plan (SIP)[1] and feeds into the performance assessment of the near field environment and overall repository. The approach taken by the SIP is to combine modeling with experimentation such that the basic processes of glass reaction are examined by experimentation, while modeling extends the limited experimental information to the full range of conditions expected for the repository.

In this paper, we describe how information produced in a series of simple site-relevant experiments can be used to support model development, and in the process, identify additional areas where information is required. The purpose of the experiments is not to generate laboratory data that can be extrapolated to predict glass performance, but to provide insight as to how glass reacts under potential repository conditions. Of particular interest is to combine information gained from analysis of both solution and the reacted glass so the complete system can be studied. Emphasis is placed on the distribution of radionuclides between the solution, the reacted glass, and other test components to assist in repository performance assessment.

EXPERIMENTAL

The experiments consisted of a series of static, batch tests terminated at time periods between 14 and 278 days. The tests were performed with as-cut monoliths of simulated SRL 165 frit based glass (Table 1), at a glass surface area/leachant volume ratio (SA/V) of 30 m^{-1}. The tests were performed in 304L type stainless steel vessels at a temperature of 90°C with J-13 water that had been preequilibrated with tuff at 90°C. The experiments were conducted with and without a polished tuff water present in the bottom of the test vessel. The results described herein are from those tests with tuff present and the complete experimental details are presented elsewhere.[2]

Table 1. Compositions of the Glass

Formula	SRL 165[a] Oxide wt %	Cation wt %
Al_2O_3	4.08	2.16
$^{241}Am_2O_3$	6.28E-4[c]	5.71E-4
B_2O_3	6.76	2.10
BaO	0.06	0.05
CaO	1.62	1.16
CeO_2	<0.05	<0.041
Cr_2O_3	<0.01	<0.007
Cs_2O	0.072	0.07
Fe_2O_3	11.74	8.21
La_2O_3	<0.05	<0.043
Li_2O	4.18	1.94
MgO	0.70	0.42
MnO_2	2.79	1.76
MoO_3	<0.01	<0.007
Na_2O	10.85	8.05
Nd_2O_3	<0.05	<0.043
NiO	0.85	0.67
$^{237}NpO_2$	2.62E-2[c]	2.31E-2
P_2O_5	0.023	0.01
$^{239}PuO_2$	2.2E-2[c]	1.94E-2
SiO_2	52.86	24.71
SrO	0.11	0.08
TiO_2	0.14	0.08
UO_2	0.92	0.81
ZnO	0.04	0.03
ZrO_2	0.66	0.49
TOTAL	98.45	

At the end of each test period, the solutions were analyzed for cations, anions, pH, carbon, and actinides, while the reacted glasses were analyzed using optical microscopy, scanning electron microscopy (SEM), secondary ion mass spectroscopy (SIMS), ion microprobe (IM), resonant nuclear reaction spectroscopy (RNRS), and analytical electron microscopy (AEM). AEM combines transmission electron microscopy with nanoprobe resolution energy dispersive X-ray spectroscopy (EDS) and electron diffraction to identify crystalline phases that form as the glass reacts. Detailed analyses are presented for samples reacted for 56, 91, and 278 days.

RESULTS AND DISCUSSION

The releases of Si, Na, B, Li, and several actinide elements from the glass, normalized to the glass surface area and elemental mass fraction are shown in Table 2. The elemental release data are typical for low SA/V experiments done for relatively short periods of time and indicate that the alkalis and boron display the largest release at a rate that gradually decreases with time. For this set of conditions (tuff present), B release is slightly less than Li through 91 days and slightly greater at 278 days, while Na and Si release are reduced compared to B and Li.

For the actinide elements, distribution between the metal components, the solution, and the tuff wafer was determined with the sum from each source used to calculate the normalized release. The total releases of U, Np, and Pu were intermediate between that of Si and Li, while the total Am release was less than Si. The distribution breakdown was actinide dependent, with U and Np being associated with both the solution and the metal vessel, while Pu and Am had a greater fraction of release associated with the metal. The Pu and Am in solution was significantly reduced after filtration with a 50 Å filter and thus must be associated with colloidal material.

Table 2. Normalized Elemental Release During Leaching

Time Period (days)	Normalized Release (gm/m^2) Li	B	Na	Si
56	3.2	2.5	1.8	1.8
91	4.9	4.6	2.5	3.0
278	7.8	10.0	3.8	2.6
Time Period (days)	**Normalized Release (gm/m^2) U**	**Np**	**Pu**	**Am**
56	1.2	0.7	0.7	0.3
91	2.5	2.5	2.0	0.4
278	3.9	5.2	5.3	1.5

From the solution data alone, it is difficult to speculate as to what processes are controlling the glass reaction; however, the data demonstrate gross release trends and indicate which elements go into solution and which remain associated with the reacted glass. A mass balance must exist between nonreacted glass and the solution/reacted glass combination.

Optical microscopy of the glass surfaces was performed to characterize gross reaction trends and to identify areas of interest for more detailed examination. As the reaction time increases, the appearance of the sample changes from being black and reflective with sharp edges retained on the as-cut surfaces, to gray, nonreflective, and fairly uniform. The 56-day sample had a duality in appearance, with some regions retaining the reflective nonreacted appearance, and other regions appearing splotchy and less reflective. Both the 91- and 278-day samples had uniformly gray surfaces characteristic of reacted glass.

SEM examination of the glass revealed that after 56 days the reflective areas had retained a smooth appearance typical of a nonreacted surface, but with the sharp edges have rounded somewhat (Fig. 1a). The splotchy areas showed the development of a cardhouse structure on the smooth surface (Fig. 1b). By 278 days, the cardhouse structure completely covered the surface and little evidence of the original surface roughness remained (Fig. 1c). Isolated precipitates rich in Ca and U were noted on the surface, but these were too small to be completely characterized and identified.

In thick flat cross-section, SEM examination of the reacted layer showed a thin banding on the original glass (Fig. 1d). Two distinct bands were present over the entire surface, with a total thickness of approximately 1 μm after 278 days. The outer band had a fairly constant reflected electron density, but appeared more porous than the original glass. The inner band, which was adjacent to the glass, also had a uniform contrast, but a low reflected electron density. The banded structure became apparent after 91 days. EDS analysis of the banded structure was difficult because the areas sampled by the electron beam were generally larger than the bands being analyzed. However, the outer band gave a total X-ray count rate similar to the glass, and compared to the glass was depleted in Na, Si, Al, and Ni, while enriched in Mg, Ca, Mn, Fe, and Zr. The inner band gave a very low X-ray count rate with the elemental composition being similar to the glass. Of the actinides, only U could be detected in the layer and it was depleted with respect to the glass.

The SEM examination indicated that a more detailed characterization of the layer was required to determine the structure and composition of the bands. AEM was utilized to provide the required detail. Electron transparent thin sections of the reacted glass were prepared using an ultramicrotomy procedure specifically developed for preparation of sections of fine-grained geological materials.[3] Small fragments of the glass with the surface layer intact were removed from a bulk specimen using a diamond blade. Care was

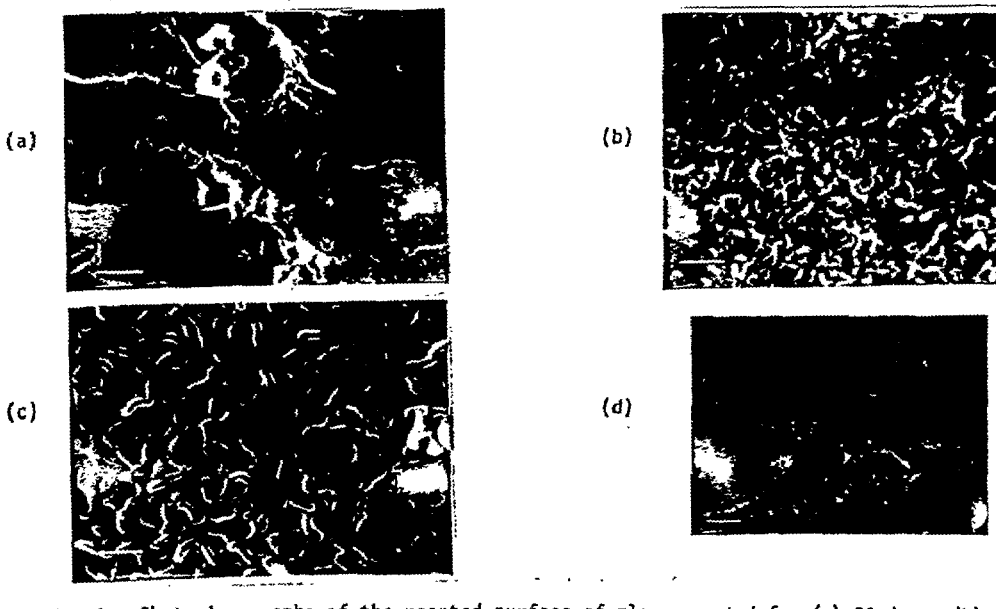

Fig. 1. Photomicrographs of the reacted surface of glass reacted for (a) 56 days, (b) 91 days, and (c) 278 days; (d) cross-section of glass reacted for 278 days

taken to select fragments less than 100 μm in size with as little unreacted glass as possible in order to minimize fragmentation of the brittle glass during sectioning. The selected fragment was mounted in epoxy or acrylic resin in an orientation which would yield cross-sectional slices containing both the surface layer and unreacted glass. A diagram of an ideal sample is shown in Fig. 2.

Brightfield transmission electron micrographs of glass reacted for 56, 91, and 278 days are shown in Fig. 3. Note the dramatic improvement in detail that can be observed in the electron transparent sections. After 56 days, a single band exists. This band is a layer with a distinct structure ~0.2 μm thick and remains firmly attached to the unreacted glass (Fig. 3a). Iron has begun to segregate toward the center of the layer where it forms a dark stain and no evidence of crystallinity can be detected throughout the layer. No evidence for a precipitated metal oxide film on the outer surface is observed. The sample was taken from a reflective nonreacted appearing region of the glass surface. The interface between the layer and the glass is fairly regular and the circular areas of contrasting electron density likely result from in-situ hydrolysis of the silicate network.

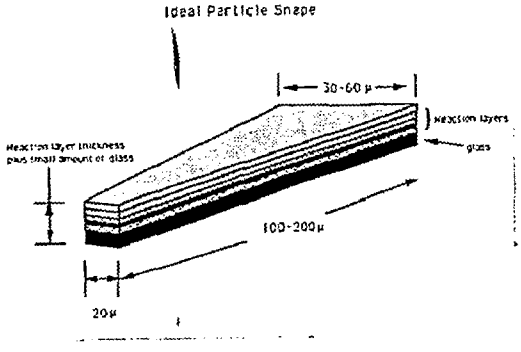

Fig. 2. Schematic drawing of an ideal sample of reacted glass for thin-section preparation

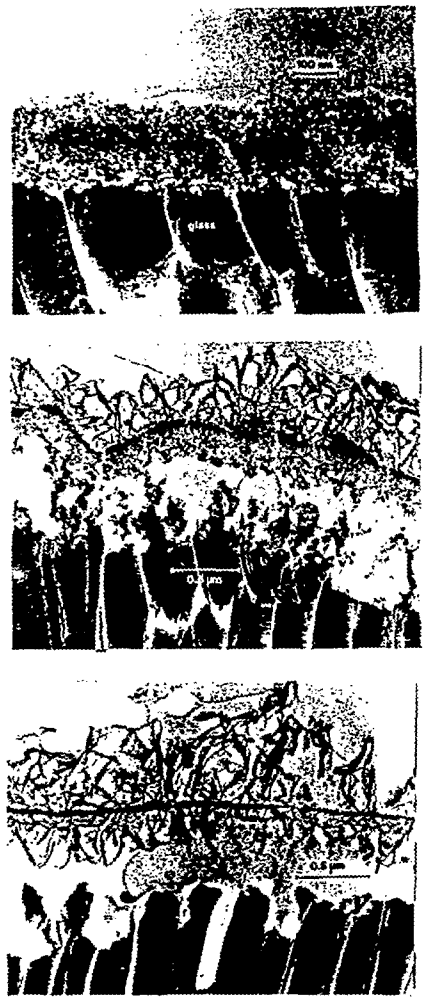

Fig. 3. Brightfield electron micrographs of cross-sections of glass reacted for (a) 56 days, (b) 91 days, and (c) 278 days

After 91 days the dual band structure becomes apparent. Iron has segregated into a well defined iron oxide "backbone" at the center of the outer band (Fig. 3b). This iron-rich region also shows an enrichment of calcium and zirconium. The outer band is actually composed of two layers that form on either side of the "backbone". The inner half

of the band retains textural characteristics of the 56-day sample, but the outer half is dominated by a lath-like material identified as smectite clay by electron diffraction, lattice fringe imaging, and quantitative EDS.[4] There is evidence that smectite is beginning to form on the inner half of the band also. The unreacted glass is now separated from the outer band by an open region that contains stringers of partially reacted glass. The open region is the second band identified in the SEM image. The open region contains solution during the glass reaction which is replaced by epoxy during sample preparation. The glass retreats from the outer band by continued reaction of the underlying glass. The thickness of the outer band itself is about 0.8 μm, while the distance between the outer surface of the band and the unreacted glass is 1.2 μm. Compared to the 56-day sample, the hydrolysis of the glass network is now occurring as the solution between the layer and the glass reacts with the glass.

After 278 days the banded structure is now mature with smectite laths dominating both the inner and outer regions on either side of the "backbone". The thickness of the outer band reaches up to 1.0 μm, while the total thickness from the outer surface of the "backbone" structure to the glass is about 1.3 μm. The outer band has completely separated from the glass and the reaction continues between the inner solution and the glass.

Compositional variations within these reacted structures ("backbone" and associated layers) were examined using quantitative EDS and the results are shown in Table 3. Comparison of the compositions of the outer vs. inner portions of the outer band in the 91- and 278-day samples suggest that element abundances correlate with the observed structural features (columns 4 through 7). For example, Mg, Mn, Ni, and Fe increase with layer silicate formation in the outer portion of the 91 day sample, while Si and Ca abundances decrease (cf. columns 2 and 5). These compositional trends continue with time. After 278 days the inner portion of the band has converted to layer silicates and as a result, Mg, Mn, and Ni abundances increase, and Si and Ca abundances decrease (cf. columns 3 and 6). At 278 days, both the appearance and composition of the inner and outer portions of the outer band are similar.

SIMS has also been performed on all samples. The results reinforce the compositional information provided by solution analysis and EDS, with additional information being obtained regarding Li and B. The sputtered area was large with respect to the features shown in the AEM images. Thus, the depth profile information represents a

Table 3. Composition of Glass and Reacted Layers (Normalized Element Wt%)[a]

	1	2	3	4	5	6	7
Mg	--	1.89	2.80	0.48	2.13	3.41	3.74
Al	8.24	12.68	13.85	12.51	13.40	14.94	15.65
Si	45.47	45.16	38.89	51.35	41.83	40.44	40.16
Ca	2.83	1.94	0.58	2.89	0.22	0.29	0.12
Ti	0.36	0.11	-	0.12	-	-	-
Mn	1.10	6.84	9.61	5.20	8.61	8.87	8.92
Fe	41.89	27.84	30.18	25.99	29.47	28.80	28.15
Ni	0.13	3.54	4.10	1.48	4.35	3.25	3.26

1. Bulk layer after 56 days (Fig. 2a).
2. Bulk layer after 91 days (Fig. 2b).
3. Bulk layer after 278 days (Fig. 2c).
4. Lower portion of leach layer after 91 days.
5. Upper portion of leach layer after 91 days.
6. Lower portion of leach layer after 278 days.
7. Upper portion of leach layer after 278 days.

[a]The composition of the layers were normalized to 100% of the elements analyzed. Oxygen and Na were not analyzed using AEM.

composite, and sharp interfaces are not observed.[2] Selected profiles are shown in Fig. 4. Here it is seen that in the 56-day sample, where the layer/glass interface is fairly uniform, depletion of Li exceeds that of B and Na. Each of these elements show a nearly complete depletion in the outer ~0.2 μm which corresponds to the thickness of the completely hydrolyzed layer shown in Fig. 3a. However, partial depletion for each element is observed further into the glass. Thus, it is likely that reaction of the glass has occurred past the glass/layer boundary, and only when the silicate network is restructured can textural differences be observed in the TEM. These SIMS profiles are consistent with the solution data where $(NL)_{Li} > (NL)_{B,Na}$, and which require a layer thickness greater than 0.2 μm to account for Li loss from the glass.

Profiles taken for the longer term samples[2] show similar shapes as the 56-day profiles, but become more difficult to interpret due to the gap that exists between the layer and the glass and the uneven nature of the glass stringers (Figs. 3b and 3c). Still, there is evidence that Li, Na, and B depletion extends further into the glass than that measured in Figs. 3b and 3c.

To further investigate the reaction process occurring as the glass etches, RNRS was conducted. The RNRS technique is based on a nuclear reaction that occurs between 6.3 Mev nitrogen ions and hydrogen which results in the emission of a gamma ray. By calculating the energy loss of an incident nitrogen ion beam as it penetrates the sample and measuring the emitted gamma ray intensity, a concentration vs. depth profile can be obtained by varying the incident nitrogen energy. Based on the structure of the reacted layers, the stopping power will be fairly uniform in the

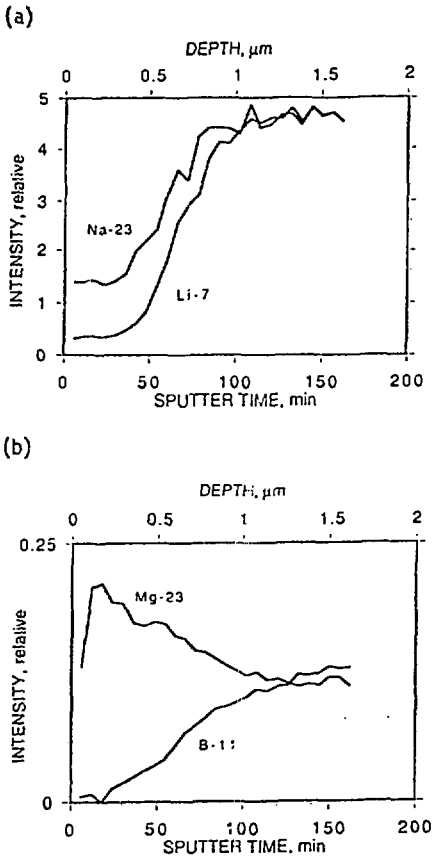

Fig. 4. SIMS profile of the 56-day sample (a) Li, Na; (b) Mg, B

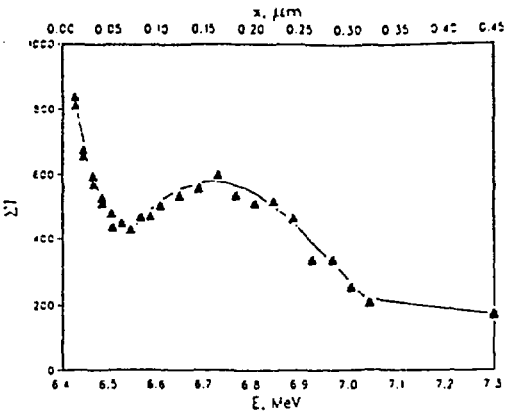

Fig. 5. RNRS profile showing the hydrogen concentration in the layer and reacted glass for the 56-day sample

56-day sample, but may be quite complicated in the longer term samples, and could result in an underestimation of the depth of H penetration. As shown in Fig. 5 for a sample reacted for 180 days, it appears that H has penetrated into the glass to about 0.5 μm while the measured layer thickness is only 0.2 μm. The RNRS profiles reinforce the previous contention that partial hydrolysis occurs in advance of the restructuring front. However, additional RNRS profiling will have to be done to establish whether water diffusion penetrates beyond the ion exchange front.

A description of the glass reaction process can be gained by combining the solution and structural data. At 56 days, the amount of glass that must have reacted to give $(NL)_{Li}$ of 3.2 g/m^2 is 1.1 μm, assuming complete Li depletion. The measured layer thickness is only 0.2 μm. Hence, the replacement of glass with layer is not isovolumetric. This is clearly seen in Fig. 1d where the layer generated within a crack in the glass does not completely fill the void. Reaction of the glass is occurring at two fronts. At the interface between the layer and glass, preferential depletion of Li, B, and Na occurs as the water penetrates glass. This region begins at the circular areas of varying contrast shown in Fig. 3a. The SIMS results (Fig. 4a) show that Li is depleted to a depth of about 0.75 μm. However, the partial Li, Na, B depletion does not account for the entire discrepancy, so the glass must also be reacting at the solution/layer interface where etching of the layer occurs. Note, as the etching occurs, there is no apparent precipitation of insoluble metals or metal oxides directly onto the layer surface. Iron, while enriched, is nearly uniformly spread throughout the layer, while Ni and Mn are noticeably depleted in the layer.

By 91 days, however, evidence for precipitation does exist with smectite eventually covering the entire surface. The iron rich "backbone" now marks the condensation of Fe, Ca, and Zr within the layer that was just beginning to occur at 56 days. Smectite, as it forms from the 56-day layer excludes Fe, Ca, and Zr from its structure and incorporates Mn and Ni from solution. Surprisingly, by 91 days, the position of the surface at 56 days becomes marked by the "backbone" and the glass continues to react via a partial hydrolysis which releases Li > B > Na (cf. SIMS and solution results), and by an etching process of the partially hydrolyzed glass.

After 278 days, complete transformation of the 56-day structure to smectite layers formed on either side of the "backbone" has occurred. The clays on either side of the "backbone" have nearly identical composition and structure suggesting that the solution composition and precipitation processes occurring within the main solution component and the inner solution component are similar. This suggests that the clay-"backbone" structure is not impeding transport of material and does not act as a protective barrier. In fact, clear transport pathways can be observed in the "backbone" structure (Fig. 3c). The partial hydrolysis process preferentially releases Li, Na, and B from the glass such that the etching front occurs from compositionally modified glass.

Based on this description of glass reaction, it is instructive to look at the distribution of actinide elements between the glass, layer, solution, and test components. Figure 6 shows an IM profile for each actinide in the 56-day sample. Uranium and Np are depleted from the outer 0.2 μm layer, Pu is fairly constant from the layer to the glass, while Am is enriched in the outer portion of the layer. Similar trends exist through 278 days. Each actinide element presumably is released from the glass structure after complete hydrolysis of the glass occurs. In the 56-day sample, hydrolysis occurs at the layer/solution interface and the layer/glass interface. Uranium and Np are released at the layer/glass interface, and are partially depleted in the layer. Both have (NL) values less than Li. Plutonium has an (NL) less than U, is not depleted from the layer, and thus must be released primarily via surface etching. Americium also is not depleted in the layer, but is enriched at the outer surface. Americium must be released due to etching at the outer surface followed by precipitation back onto the glass yielding a low (NL) value.

At longer time periods, complete hydrolysis occurs at the inner solution/glass interface. Neptunium and U are depleted in the layer and have (NL) values only slightly less than Li. The amount of Pu in the layer remains constant with time and the $(NL)_{Pu}$ is similar to U and Np. This indicates as Pu is released from the glass it does not further accumulate in the layer but passes into solution. Americium, however, continues to accumulate on the outer surface of the layer and the $(NL)_{Am}$ is less than the other actinides. It is important to note that most of the Pu and Am measured in the solution component is associated with the filterable fraction and is associated with colloidal material that forms as the glass reacts (see Ref. 2).

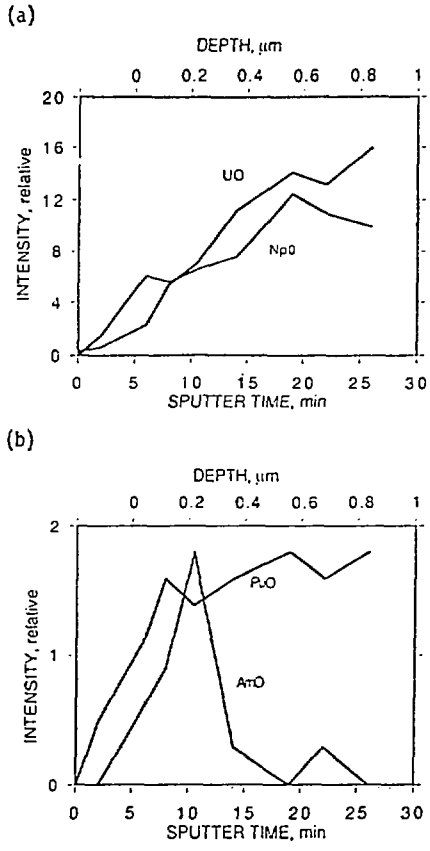

Fig. 6. Ion microprobe profiles of actinides in the reacted 56-day sample

IMPLICATIONS FOR MODELING

The approach being used by the YMP to model glass reaction utilizes the EQ3/6 computer code to (1) model the glass dissolution, and (2) equilibrate the resulting solution by generating secondary phases. The glass dissolution rate is modeled by Eq. 1 which includes the term (1 - Q/K) describing the influence of the solution on the reaction affinity:

$$\left[\frac{dC_i}{dt} = \frac{SA}{V} \nu_i k_m (1 - Q/K) \right] \quad (1)$$

where C_i is the solution concentration of species i, SA/V is the glass surface area/leachant volume ratio, ν_i is a stoichiometric factor, k_m is the maximum forward reaction rate, and (1 - Q/K) is the

affinity term. Both the solution volume and solution composition influence the rate of glass dissolution. The rate coefficient, k_m, depends on the glass phase reacting and may differ for fresh glass and glass from which the alkali metal ions (and boron) have been leached. The modeling approach taken, therefore, requires a knowledge of the glass composition (pristine or partially hydrated) which determines the observed reaction rate, the appropriate SA/V of the reacting system, and the secondary phases formed which control the reaction affinity term.

The present results support this approach in that there is evidence that etching of partially hydrated glass occurs. Up to 56 days, etching occurs in concert with hydrolysis at the layer/glass interface. After 56 days, the etching occurs between the inner solution and the partially hydrolyzed glass. The "backbone" structure grows as phases precipitate from the inner and outer solution. Application of Eq. 1 requires knowledge of the composition of the solution in contact with the dissolving glass or altered glass surface. This information is used to calculate "Q" in the affinity term, the activity product for the glass dissolution reaction. In the present experiments, two solution volumes exist, one on each side of the layer. However, since the clay phases on both sides of the "backbone" have identical compositions, and since transport pathways through the "backbone" are evident, it is likely that the total volume can be used in calculations. The results of calculations performed using Eq. 1 and the composition of the partially hydrated glass have been presented previously,[5] and indicate that through 278 days the modeling approach is consistent with the experimental data.

However, questions remain as to how to extend these calculations to predict long-term glass performance. These include (1) What is the fate of the reacted layer? Will it remain weakly attached to the reacting glass surface and eventually provide a barrier to mass transport, or will it spall from the glass surface and be available for transport as colloidal material? Results from the present experiments suggest that some spallation occurs because >99% of the Am and Pu in the solution are associated with particulates. If spallation does occur, will the layer reform and how will the glass reaction continue? (2) What is the size distribution of actinide-bearing phases in solution, and what phases are the actinides associated with? Will actinides that are present in amorphous solids or loosely bound as sorbed species be returned to solution with aging and crystallization? (3) Will other secondary phases form as the solution becomes concentrated in leached glass components, thus changing the affinity for reaction? Will the inner and outer solution compositions remain the same or will the inner solution become more concentrated resulting in different phases forming on each side of the "backbone"? (4) Will the partially hydrated zone continue to grow thereby releasing alkali to solution in a noncongruent fashion? Will such noncongruent release require a more sophisticated model?

The answer to these questions are best addressed by performing experiments of longer duration or under conditions that accelerate the reaction process. Such data are necessary for the eventual validation of the modeling approach being taken by the YMP, and for credible performance assessment of the repository.

ACKNOWLEDGMENTS

Work support by the U.S. Department of Energy, Office of Civilian Radioactive Waste Management, Yucca Mountain Project, under subcontract to Lawrence Livermore National Laboratory, SANL-110-003; and by the Office of Environmental Restoration and Waste Management, under Contract W-31-109-ENG-38.

REFERENCES

1. R. D. AINES, "Plan for Glass Waste Form Testing for NNWSI", UCID-21190, Lawrence Livermore National Laboratory (1987).

2. W. L. EBERT, J. K. BATES, and T. J. GERDING, "The Reaction of Glass during Gamma Irradiation in a Saturated Tuff Environment, Part 4: SRL 165, ATM-1c, and ATM-8 Glasses at 1E3 R/h and 0 R/hr," ANL-90/13, Argonne National Laboratory (1990).

3. J. P. BRADLEY, "Analysis of Chondritic Interplanetary Dust Thin-Sections," Geochim. Cosmochim. Acta, 52, 889 (1988).

4. J. P. BRADLEY and J. K. BATES, "Leached Nuclear Waste Glasses: Ultramicrotomy and Analytical Electron Microscopic Characterization," Proc. of the 12th Int. Congress for Electron Microscopy, Seattle, WA, August 13-17, 1990, pp. 444-445 (1990).

5. W. L. BOURCIER, "Overview of Chemical Modeling of Nuclear Waste Glass Dissolution," Scientific Basis for Nuclear Waste Management XIV, Materials Research Society, Boston, MA, November 26-29, 1990 (in press).